Journal of Molecular Structure 1094 (2015) 237–245

Contents lists available at ScienceDirect

Journal of Molecular Structure

journal homepage: www.elsevier.com/locate/molstruc

Synthesis, characterization, antibacterial activity and quantum chemical studies of N'-Acetyl propane sulfonic acid hydrazide

Saliha Alyar [a,*], Hamit Alyar [b], Ummuhan Ozmen Ozdemir [c], Omer Sahin [d], Kerem Kaya [d], Neslihan Ozbek [e], Ayla Balaban Gunduzalp [c]

[a] Department of Chemistry, Science Faculty, Karatekin University, Çankırı, Turkey
[b] Department of Physics, Science Faculty, Karatekin University, Çankırı, Turkey
[c] Department of Chemistry, Science Faculty, Gazi University, Ankara, Turkey
[d] Department of Chemistry, Faculty of Science and Letters, Istanbul Technical University, Istanbul, Turkey
[e] Department of Chemistry Faculty of Education, Ahi Evran University, Kırşehir, Turkey

HIGHLIGHTS

- Synthesis of N'-Acetyl propane sulfonic acid hydrazide (*Apsh*).
- Characterization of *Apsh*.
- ^{1}H and ^{13}C shielding tensors for crystal structure with GIAO/DFT/B3LYP/6-311++G(d,p) methods.
- The vibrational band assignments for crystal structure with B3LYP/6-311++G(d,p)/(SQMFF).
- Antimicrobial activities of *Apsh*.

GRAPHICAL ABSTRACT

N'-Acetyl propane sulfonic acid hydrazide has been synthesized for the first time and investigated its antibacterial activity. Also ^{1}H and ^{13}C shielding tensors for crystal structure were calculated with GIAO/DFT/B3LYP/6-311++G(d,p) methods in $CDCl_3$.

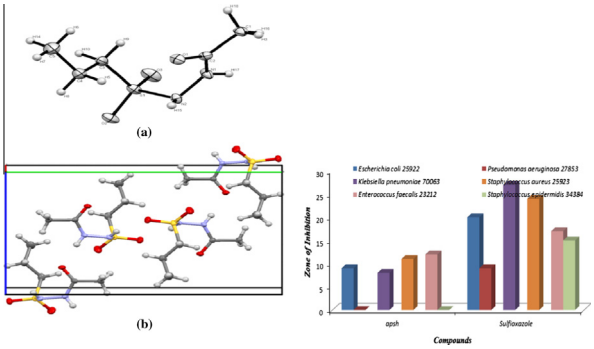

ARTICLE INFO

Article history:
Received 30 December 2014
Received in revised form 26 March 2015
Accepted 26 March 2015
Available online 6 April 2015

Keywords:
Propane sulfonic acid hydrazide
Biological activities
Antibacterial activity
X-ray
DFT

ABSTRACT

A new N'-Acetyl propane sulfonic acid hydrazide, $C_3H_7—SO_2—NH—NH—COCH_3$ (Apsh, an sulfon amide compound) has been synthesized for the first time. The structure of *Apsh* was investigated using elemental analysis, spectral (IR, $^{1}H/^{13}C$ NMR) measurements. In addition, molecular structure of the Apsh was determined by single crystal X-ray diffraction technique and found that the compound crystallizes in monoclinic, space group P 21/c. ^{1}H and ^{13}C shielding tensors for crystal structure were calculated with GIAO/DFT/B3LYP/6-311++G(d,p) methods in $CDCl_3$. The structure of Apsh is optimized using Density Functional Theory (DFT) method. The vibrational band assignments were performed at B3LYP/6-311++G(d,p) theory level combined with scaled quantum mechanics force field (SQMFF) methodology. The theoretical IR frequencies are found to be in good agreement with the experimental IR frequencies. Nonlinear optical (NLO) behaviour of Apsh is also examined by the theoretically predicted values of dipole moment (μ), polarizability (α_0) and first hyperpolarizability (β_{tot}). The antibacterial activities of synthesized compound were studied against Gram positive bacteria: *Staphylococcus aureus* ATCC

* Corresponding author.

http://dx.doi.org/10.1016/j.molstruc.2015.03.059
0022-2860/

25923, *Enterococcus faecalis* ATCC 23212, *Staphylococcus epidermidis* ATCC 34384, Gram negative bacteria: *Eschericha coli* ATCC 25922, *Pseudomonas aeruginosa* ATCC 27853, *Klebsiella pneumoniae* ATCC 70063 by using microdilution method (as MICs) and disc diffusion method.

Introduction

The importance of sulfonamide was realized [1] when sulfonylamide, a key analogue of sulfonamide, was reported [2] to be the first antibacterial drug. Sulfonamides were the first effective chemotherapeutic agents employed systematically for the prevention and the cure of bacterial infections in humans and other animal systems [3,4]. Later on, many thousands of molecules containing the sulfanilamide structure have been created since its discovery, yielding improved formulations with greater effectiveness and less toxicity. Sulfa drugs are still widely used for conditions such as acne and urinary tract infections, and are receiving renewed interest for the treatment of infections caused by bacteria resistant to other antibiotics. Also, a number of other activities, some of which have been recently observed, include endothelin antagonism, anti-inflammatory activity, tubular transport inhibition, insulin release, carbonic anhydrase and saluretic action, among others [5].

In our previous studies, aliphatic/aromatic bis sulfonamides were synthesized and tested for antimicrobial activity [6–9]. Also, we have reported conformational analysis and vibrational spectroscopic investigation of the methanesulfonic acid hydrazide [10] methanesulfonic acid 1-methylhydrazide [11] some methane/ethane sulfonylhydrazone derivatives [12–15]. In this work, N'-Acetyl propane sulfonic acid hydrazide *(Apsh)* was synthesized and characterized by using elemental analyses, FT-IR, NMR, spectrometric methods. *Apsh* has also been characterized by single crystal X-ray diffraction. ^{1}H and ^{13}C shielding tensors for crystal structure were calculated with GIAO/DFT/B3LYP/6-311++G(d,p) methods in $CDCl_3$. The vibrational band assignments were performed at B3LYP/6-311++G(d,p) theory level combined with scaled quantum mechanics force field (SQMFF) methodology. The antibacterial activities of synthesized compounds were studied against Gram positive bacteria: *Staphylococcus aureus* ATCC 25923, *Enterococcus faecalis* ATCC 23212, *Staphylococcus epidermidis* ATCC 34384, Gram negative bacteria: *Eschericha coli* ATCC 25922, *Pseudomonas aeruginosa* ATCC 27853, *Klebsiella pneumoniae* ATCC 70063 by using microdilution method (as MICs) and disc diffusion method.

Experimental

Physical measurements

The crystal structure of N'-Acetyl propane sulfonic acid hydrazide (Apsh) was determined by using a on a Bruker D8 Venture. The solvents used were purified and distilled according to routine procedures. Propane sulfonyl chloride and hydrazine hydrate were commercial products (purum). ^{1}H and ^{13}C-NMR spectra of dimethylsulfoxide-d_6 (DMSO-d_6) solutions of the compounds were registered on a Bruker WM-400 spectrometer (400 MHz) using tetra methyl silane as internal standard. The infrared spectra of the compounds as KBr-disks were recorded in the range of 4000–400 cm^{-1} with a Mattson 1000 FT spectrometer. Melting points of compound was determined with a Gallenkamp melting point apparatus. The microdilusion broth and disc diffusion method were used to determine the antibacterial activity of compounds against Gram positive bacteria: *S. aureus* ATCC 25923, *E. faecalis* ATCC 23212, *S. epidermidis* ATCC 34384, Gram negative bacteria: *E coli* ATCC 25922, *P. aeruginosa*ATCC 27853, *K. pneumoniae* ATCC 70063.

Synthesis of N'-Acetyl propane sulfonic acid hydrazide

The nucleophilic substitution reaction of the hydrazine hydrate with propane sulfonyl chloride was carried out as follows:

An ethanol solution of propane sulfonyl chlorides ($C_3H_7SO_2Cl$) was added dropwise to the ethanol solution of hydrazine hydrate (0.12: 0.62 equiv), maintaining the temperature between 10–12 °C. Then, the reaction mixture was stirred for 1 h at room temperature. After the completion of the reaction, the solvent was removed under vacuum and the viscose residue was taken to ether phase using a continuous extraction method. Then the ether was removed with rotary evaporator. The resulting product was boiled with ethyl acetate and then allowed to stand in the freezer. Bright transparent crystals were obtained after a few weeks. Calc. for $C_5H_{12}N_2O_3S$: C, 33.32; H, 6.71; N, 15.54; O, 26.63; S, 17.79% Found: C, 32.87; H, 6.48; N, 14.98; O, 25.93; S, 17.20%. Yield: 70%, M.p.114–116 °C.

Crystallography

Crystallographic data of the compound were recorded on a Bruker D8 Venture X-ray diffractometer equipped with PHOTON 100 CMOS detector using graphite monochromatized MoKα radiation (λ = 0.71073 Å), and using only ω-scan mode. The empirical absorption corrections were applied by multi-scan via Bruker, SADABS software [16]. The structures were solved by the direct methods and refined by full-matrix least-squares techniques on F^2 using the solution program SHELXS-97 and refined using SHELXL-2014/6. All non-hydrogen atoms were refined with anisotropic displacement parameters. The molecular structure plots were prepared using Mercury CSD 2.4 [17]. The crystal and instrumental parameters used in the unit-cell determination and data collection are summarized in Table 1 for the compounds.

Theoretical calculations

Because of the effective bioactivities of N'-Acetyl propane sulfonic acid hydrazide the three dimensional conformation of the molecule was also determined as it will be able to give important previews about molecular behaviour in gas and solution forms. The molecular geometry optimizations, HOMO, LUMO frontier molecular orbital energy, nonlinear optical (NLO) activity and vibration frequency calculations were performed with the Gaussian 03 W software package by using DFT approaches in addition to the determination of crystal structure [18]. The split valence 6-311++G (d, p) basis set was used for the expansion of the molecular orbital [19]. The geometries were fully optimized without any constraint with the help of an analytical gradient procedure implemented within the Gaussian 03 W program. All the parameters were allowed to relax and all the calculations converged to an optimized geometry which corresponds to a true energy minimum as revealed by the lack of imaginary values in the wave number calculations. The ^{1}H and ^{13}C NMR chemical shifts of the compounds were calculated in $CDCl_3$ using the GIAO

Table 1
Crystal data and structure refinement details for Apsh molecule.

	1
Empirical formula	$C_5H_{12}N_2O_3S$
Formula weight	180.23
T(K)	100
λ(Å)	0.71073
Crystal system, space group	Monoclinic, P 21/c
Unit cell dimensions: (Å, °)	
a	6.2754(12)
b	15.240(3)
c	9.3007(18)
β	94.738(6)
V(Å3)	886.4(3)
Z	4
Absorbtion coefficient (mm^{-1})	0.331
Dcalc (Mg/m^3)	1.358
F(000)	388.0
Crystal size (mm)	0.020x0.200x0.500
θ Range for data collection (°)	2.57–27.54°
Index ranges	$-8 \leqslant h \leqslant 8$ $-19 \leqslant k \leqslant 19$ $-10 \leqslant l \leqslant 12$
Reflections collected	20350
Independent reflections	2028
Data/parameters	2028/111
Max. and min. transmission	0.993, 0.852
Final R indices [$I \geqslant 2\sigma(I)$]	$R1$ = 0.0787, $wR2$ = 0.2186
R indices (all data)	$R1$ = 0.0807,$wR2$ = 0.2193
Goodness-of-fit on F^2	1.333
Largest difference in peak and hole (e $Å^{-3}$)	1.166/−0.507

method. The vibrational band assignments were performed at B3LYP/6-311++G (d,p) theory level combined with scaled quantum mechanics force field (SQMFF) methodology.

Procedure for antibacterial activity

S. aureus ATCC 25923, *E. faecalis* ATCC 23212, *S. epidermidis* ATCC 34384, *E coli* ATCC 25922, *P. aeruginosa* ATCC 27853, *K. pneumoniae* ATCC 70063by cultures were obtained from Hacettepe University, Department of Medical Microbiology. Bacterial strains were cultured overnight at 37 °C in Nutrient Broth. During the survey, these stock cultures were stored in the dark at 4 °C.

Disc diffusion method

The synthesized compound was dissolved in dimethylsulfoxide (20% DMSO) to a final concentration of 3.0 mg mL^{-1} and sterilized by filtration by 0.45 μm millipore filters. Antimicrobial tests were then carried out by the disc diffusion method using 100 μL of suspension containing 10^8 CFU mL^{-1} bacteria spread on a nutrient agar (NA) medium. The discs (6 mm in diameter) were impregnated with 25 μL of each compound (150 μg/disc) at the concentration of 3.0 mg mL^{-1} and placed on the inoculated agar. DMSO impregnated discs were used as negative control. Sulfioxazole (300 μg/disk) were used as positive reference standards to determine the sensitivity of one strain/isolate in each microbial species tested. The inoculated plates were incubated at 37 °C for 24 h for bacterial strains isolates. Antimicrobial activity in the disc diffusion assay was evaluated by measuring the zone of inhibition against the test organisms. Each assay in this experiment was repeated twice [20].

Micro dilution assays

The minimal inhibition concentration (MIC) values, except one, were also studied for the microorganisms sensitive to at least one of the five compounds determined in the disc diffusion assay. The inocula of microorganisms were prepared from 12 h broth cultures and suspensions were adjusted to 0.5 McFarland standard turbidity. The test compounds dissolved in dimethylsulfoxide (DMSO) were first diluted to the highest concentration (3000 μg mL^{-1})to be tested, and then serial, two-fold dilutions were made in a concentration range from 46.875 to 3000 μg mL^{-1} in 10 mL sterile test tubes containing nutrient broth. The MIC values of each compound against bacterial strains were determined based on a micro-well dilution method [21]. The 96-well plates were prepared by dispensing 95 μL of nutrient broth and 5 μL of the inoculums into each well. One hundred μL from each of the test compounds initially prepared at the concentration of 3000 μg mL^{-1} was added into the first wells. Then, 100 μL from each of their serial dilutions was transferred into eight consecutive wells. The last well containing 195 μL of nutrient broth without compound, and 5 μL of the inoculums on each strip, was used as negative control. The final volume in each well was 200 μL. The contents of the wells were mixed and the micro plates were incubated at 37 °C for 24 h. All compounds tested in this study were screened twice against each microorganism. The MIC was defined as the lowest concentration of the compounds to inhibit the growth of microorganisms.

Results and discussion

Crystal structure analysis

Molecular structure with the atom-numbering scheme of *Apsh* was given in Fig. 1(a). Crystal data and structure refinement parameters of *Apsh* were given in Table 1. Experimental geometric parameters are given in Table 2. The compound crystallised in the P 1 21/c 1space group. The length of the C—O bond is 1.230 Å. Unit cell content indicating the crystal packing structure of the molecule is given in Fig. 1(b). The S—O and S—N bond distances lie within expected range of 1.431(4)–1.443(3) Å and 1.654(4) Å, respectively. All bond lengths and angles for compound are consistent with those found in related compounds [22–24] (Table 2).

The characterization of compounds

Vibrational spectral analysis

The infrared spectra were recorded in the 4000–400 cm^{-1} region using KBr pellets on a MATTSON-1000 model FT-IR spectrometer. The vibrational band assignments were performed at B3LYP/6-311++G(d,p) theory level combined with scaled quantum mechanics force field (SQMFF) methodology to compare the experimental and calculated vibrational frequencies of the title compound [25]. The visual check for the vibrational band assignments were also performed by using Gauss-View program. The vibrational wavenumbers were calculated and then scaled by using the scaling factors for primitive coordinates proposed by our previous study [26]. The each vibrational modes of the studied compound were characterized by their potential energy distributions (PED) which were calculated by using SQM-FF program [27].

N—H vibrations. The N—H stretching vibration of secondary amine groups of some aliphatic sulfonamides occurs in the region 3300–3200 cm^{-1} [28]. In the present study, the strong bands at 3231 cm^{-1} (IR) assigned to the N—H stretching mode of Apsh and this band were calculated at 3541 and 3533 cm^{-1}.

The band corresponding to N—H in-plane bending vibration is expected near 1400 cm^{-1} [7,10,12,29–31]. The band observed at 1418 cm^{-1} in the FT-IR of Apsh attributed to N—H in-plane bending mode. This band was calculated at 1482 and 1365 cm^{-1}.

C—H vibrations. The C—H stretching vibrations of aliphatic compounds are observed slightly below 3000 cm^{-1}[7,10–12,31,32].

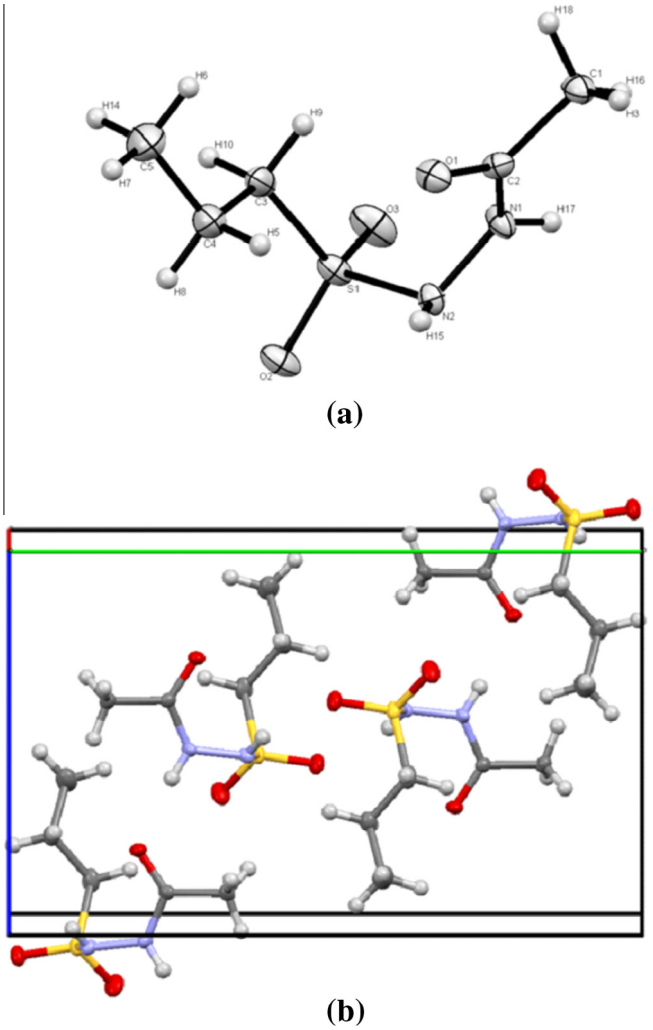

Fig. 1. The molecular structure of *Apsh* with the atom-numbering scheme; displacement ellipsoids are drawn at the 50% probability level (a) and the crystal packing (b) of *Apsh*.

The bands in the range of 2996–2902 cm^{-1} are due to C—H stretching modes of the methyl CH_3 and methylene CH_2 groups of Apsh. In fact, the assignment of the vibrations of methylene group is very difficult because of the presence of the methyl group.

The other fundamental CH_3 and CH_2 group vibrations which are CH_2 scissoring, antisymmetric or symmetric CH_3 bending, CH_2 twisting and CH_3 rocking modes appear in the expected wavenumber region of 1465–775 cm^{-1}.

C═O and S═O vibrations. The C═O carbonyl group gives rise to a strong absorption in the region 1820–1660 cm^{-1}. In this study, the C═O stretching vibration observed at 1672 cm^{-1} and calculated at 1735 cm^{-1}.

The SO_2 antisymmetric and symmetric stretching vibrations appear in the range 1330 ± 30 cm^{-1} and 1160 ± 30 cm^{-1}, both with strong intensity [33,34]. The strong band at 1305 cm^{-1} in the FT-IR spectrum assigned to SO_2 antisymmetric mode and 1100 cm^{-1} are attributed to SO_2 symmetric mode. These experimental values agree with calculated wavenumbers 1299 and 1084 cm^{-1}, respectively.

S—N and C—S vibrations. S—N stretching vibration appears in the range 905 ± 70 cm^{-1}[33]. This vibration occurs in medium band in the IR spectrum [33,34]. This band observed at 855 and 671 cm^{-1} and calculated at 832 and 653 cm^{-1}.

C—S stretching band of some methanesulfonamide derivatives in solid phase have been defined in the region of 760–780 cm^{-1} [35]. The strong band at 764 cm^{-1} in the FT-IR spectrum assigned as C—S stretching band and calculated at 682 cm^{-1}. The above conclusions are in good agreement with the literature values. The other experimental and calculated vibrational frequencies can be seen in Table 3.

NMR spectra

The NMR spectra (^1H, ^{13}C) of *Apsh* was measured and interpreted in DMSO. The ^{13}C NMR and ^1H NMR spectrum of the *Apsh* in dimethyl sulfoxide are given in Fig. 2. In order to facilitate the interpretation of the NMR spectra, quantum-chemical calculations were performed using B3LYP/6-311G++(d,p) basis set *Apsh* in DMSO phase. Isotropic shielding tensors of ^{13}C were changed into chemical shifts by using a linear relationship suggested by Blanco et al. [36]. A similar relationship proposed by Silva et al. [37] was used to obtain chemical shifts for ^1H. The experimental and calculated chemical shift values are shown in Table 4. In Table 4, the ^1H NMR spectrum of *Apsh*, H4 and H1 protons appeared at 0.85 ppm and 1.82 ppm were calculated at 1.07 ppm and 1.79 ppm. The

Table 2
Experimental and calculated structural parameters (bond length in Å, angles in °) of Apsh molecule.

Bond length			Bond angle			Bond angle		
	Exp	Calc		Exp	Calc		Exp	Calc
S1—O3	1.431(4)	1.463	O3S1O2	119.2(2)	121.3	O1C2N1	121.8(4)	123.0
S1—N2	1.654(4)	1.734	O2S1N2	103.0(2)	104.2	N1C2C1	114.6(4)	113.7
O1—C2	1.230(6)	1.211	O2S1C3	108.7(2)	108.8	C4C3H9	108.8	108.9
N1—N2	1.417(5)	1.385	C2N1N2	121.4(4)	119.6	H9C3H10	107.7	108.5
N2—H15	0.72(6)	1.015	N1N2H15	110(5)	112.7	Torsion Angle		
C1—H18	0.9800	1.091	N1N2S1	114.5(3)	117.2		Exp	Calc
C3—C4	1.528(7)	1.530	C2C1H18	109.5	108.3	C2—N1—N2—S1	96.3(5)	92.8
C4—C5	1.522(8)	1.531	C2C1H3	109.5	113.6	N2—N1—C2—C1	178.0(4)	173.8
C5—H6	0.9800	1.091	O1C2C1	123.6(4)	123.1	O2—S1—C3—C4	44.9(4)	52.17
S1—O3	1.431(4)	1.464	C4C3S1	113.8(4)	112.9			
S1—N2	1.654(4)	1.734	C5C4C3	110.6(5)	115.1			
S1—O2	1.443(3)	1.463	O3S1N2	106.6(2)	108.1			
S1—C3	1.767(5)	1.817	O3S1C3	108.9(3)	108.8			
N1—C2	1.342(6)	1.390	N1S1C3	110.1(2)	101.7			
N1—H17	0.83(8)	1.014	C2N1H17	120(5)	117.2			
C1—C2	1.508(7)	1.514	N2N1H17	116(5)	116.8			
C1—H3	0.9800	1.091	S1N2H15	115(5)	108.7			
C3—H9	0.9900	1.091	C2C1H16	109.5	108.6			

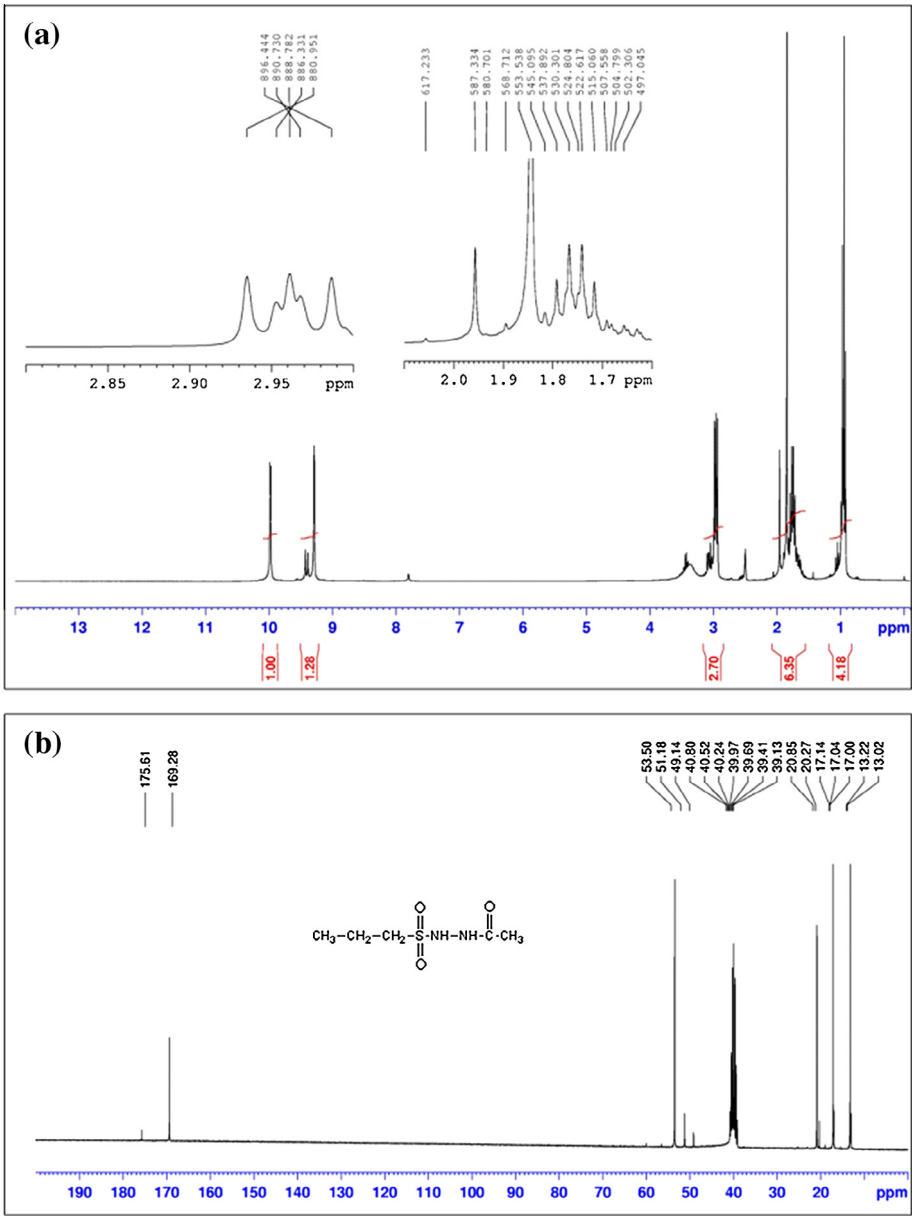

Fig. 2. (a) ^{1}H NMR of the *Apsh* and (b) ^{13}C NMR of the *Apsh.*

CH_2 protons of propyl moiety, H5 and H3 (two H intensities) are observed at 1.95, 2.98 ppm, and corresponding calculation values are 1.89 ppm, 3.44 ppm respectively. In addition, the singlet peaks N(1)H and N(2)H protons appeared at 9.27 ppm and 9.97 ppm (calculated 7.47 ppm and 5.67 ppm) respectively. The ^{13}C NMR spectrum of *Apsh,* C4 and C1 carbon signals gave the following results: 13.02 ppm and 17.04 ppm (calculated 12.52 ppm, 19.56 ppm) respectively. The ^{13}C NMR spectra of *Apsh* were assigned at δ 20.27 ppm, 53.50 ppm (calculated 19.83 ppm, 68.58 ppm respectively) for **C**5 and **C**3 carbon atoms.

Frontier molecular orbital analysis

The highest occupied molecular orbital (HOMO) and the lowest unoccupied molecular orbital (LUMO) are the very important for quantum chemistry. The HOMO and LUMO are the main orbitals in chemical stability. The HOMO represents the ability to donate an electron, LUMO as an electron acceptor representing the ability to obtain an electron. These orbitals play an important role in the electric and optical properties. The HOMO and LUMO are the main orbital taking part in chemical reaction. The HOMO energy is directly related to the ionization potential, LUMO energy is directly related to the electron affinity. The frontier molecular orbitals (HOMO and LUMO) are mostly the π-antibonding type molecular orbitals in the structure.

The energy difference between HOMO and LUMO orbital ($E_{HOMO\text{-}LUMO}$) which is called as energy band gap is a critical parameter in determining molecular electrical transport properties and electronic systems because it is a measure of electron conductivity. Also, the energy band gap helps to characterize the chemical reactivity and kinetic stability of the molecule [38].

To provide a relation between HOMO-LUMO optical band gap and nonlinear optical activity for the title compound were investigated. The energy difference $E_{HOMO\text{-}LUMO}$ was found to be 7.06 eV for Apsh molecule. The frontier molecular orbital distributions and energy levels of the HOMO-1, HOMO, LUMO and LUMO + 1orbitals, which computed at B3LYP/6–311++G(d,p) level of the title molecule are shown in Fig. 3.

Table 3
The vibrational assignments of the *Apsh* molecule by normal mode analysis based on SQM force field calculations.

Mode	Experimental	B3LYP/6-311++G(d,p)		Potential Energy Distributions (P.E.D.)
	IR	Unscaled freq	Scaled freq	Description (%)
63		3542	3541	υ (N1—H17) (99)
62	3231	3534	3533	υ (N2—H15) (99)
61		3130	2996	υ_{as} (C3—H_2) (75) + υ_{as} (C1—H_3) (24)
60		3130	2995	υ_{as} (C1—H_3) (75) + υ_{as} (C3—H_2) (24)
59		3115	2982	υ_{as} (C1—H_3) (100)
58	3223	3109	2976	υ_{as} (C5—H_3) (95)
57	2969	3095	2962	υ_{as} (C5—H_3) (86) + υ_{as} (C4—H_2) (11)
56		3075	2943	υ_{s} (C3—H_2) (67) + υ_{as} (C4—H_2) (27)
55		3064	2933	υ_{as} (C4—H_2) (58) + υ_{s} (C3—H_2) (38)
54	2878	3046	2916	υ_{s} (C1—H_3) (100)
53		3032	2902	υ_{s} (C5—H_3) (90) + υ_{s} (C4—H_2) (10)
52		3032	2902	υ_{s} (C4—H_2) (88) + υ_{s} (C5—H_3) (10)
51	1672	1780	1735	υ (C16—O1) (85) + υ (C1—C2) (3)
50	1665	1536	1482	υ (C2—N1) (15) + δ(NN—H17) (33) + δ(CN—H17) (27) + δ(NN—H15) (7)
49	1550	1504	1465	sci (C4—H_2) (48) + δ(C5—H_3) (32)
48	1456	1502	1457	γ(C5—H_3) (87)
47		1487	1454	δ(C1—H_3) (92)
46		1486	1438	δ(C5—H_3) (53) + sci (C4—H_2) (28)
45	1429	1471	1429	sci (C4—H_2) (86)
44	1399	1456	1423	γ(C1—H_3) (98)
43	1380	1426	1371	υ(C5—C4)(5) + γ(C5—H_3) (67)
42	1376	1418	1365	υ_{as}(SO_2) (15) + δ(N2—H15) (56) + δ(N1—H17) (12)
41	1355	1397	1345	γ(C5—H_3) (94)
40	1331	1381	1338	w(C4—H_2) (44) + t(C3—H_2) (23)
39		1344	1308	υ(S—O3) (15) + w (C4—H_2) (22) + t(C3—H_2) (23)
38	1305	1295	1299	υ_{as}(SO_2) (60) + δ(NN—H15) (5) + δ(SC3—H9) (4)
37	1248	1284	1248	γ(C5—H_3) (12) + w(C4—H_2) (41) + t(C3—H_2) (24)
36	1218	1260	1240	υ(C2—N1) (28) + υ(NN) (27) + υ(C2—C1) (8) + δ(NN—H17) (8) + δ(CN—H17) (5) + δ(CC—H3) (5)
35		1224	1190	γ(C5—H_3) (26) + t(C3—H_2) (43) + δ(CC—H6) (5)
34	1155	1158	1146	υ(NN) (56) + υ(C1—C2) (13) + γ(CC—H3) (7) + δ(CC—O1) (6)
33		1108	1113	υ(C3—C4) (26) + υ(C5—C4) (17) + γ(C5—H_3) (14) + δ(CC4—H6) (9) + δ(SC—H10) (7)
32	1100	1100	1084	υ_{s}(S—O3) (44) + υ_{s}(S—O2) (42)
31	1065	1082	1058	υ(C5—C4) (14) + υ(S—O3) (4) + γ(C5—H_3) (27) + δ(CC—C5) (6) + δ (CH_2—S) (15) + δ(C3—C4—H8) (8)
30	1043	1053	1034	γ(C1—H_3) (94)
29	1007	1048	1025	υ(C5—C4) (22) + υ(C3—C4) (18) + γ(C5—H_3) (22) + δ(CC5—H6) (10) + δ(SC—H10) (6) + δ(CC—H8) (5)
28	980	1005	978	υ(C1—C2) (29) + υ(C—O1) (7) + γ(C1—H_3) (33) + δ(NNC) (6) + δ(CCN) (6) + δ(NC—O1) (5)
27	940	941	920	υ(NC) (39) + γ(C1—H_3) (22) + δ(NNC) (10) + δ(CN—H17) (7) + δ(NC—O1) (6)
26	890	897	881	υ(C3—C4) (25) + υ(C5—C4) (15) + γ(C5—H_3) (30)
25		852	843	υ(C5—C4) (23) + υ(C3—C4) (14) + ρ (C3—H_2) (30)
Mode	Experimental	B3LYP/6311G(d,p)		Potential Energy Distributions (P.E.D.)
	IR	Unscaled	Scaled	Description (%)
24	855	839	832	υ(SN) (32) + υ(CS) (6) + υ(NC) (5) + γ(N12—H15) (40)
23		789	775	υ(CS) (5) + γ(C5—H_3) (25) + ρ (C4—H_2) (31) + ρ (C3—H_2) (9) + δ(CCS) (4)
22	764	689	682	υ(CS) (29)+ υ(C1—C2) (10) + δ(NC—O1) (5) + δ(O2—SN) (5) + τ(O2—SNH15) (6)+τ(OCN—H17) (5)
21	671	660	653	υ(C1—C2) (20) + υ(CS) (17) + υ(SN) (14) + δ(NCO) (10) + δ(NN—C2) (7)
20	597	616	611	υ(CS) (6) + γ(C1—H_3) (13) + τ(NC16—CH_3) (15) + τ(O1C—CH_3) (18) + τ(O1CNN) (16) + τ(O1CNH) (12)
19	555	566	553	δ(OSN) (8) + δ(SCC) (5) + δ(SNH) (5) + δ(CCO) (5) + τ(SO_2) (38)
18		546	541	δ(NN—H15) (11) + τ(SNN—H17) (17) + τ(HNNH) (25) + τ(CCN—H17) (17) + τ(O1CN—H17) (14)
17	511	508	499	υ(SN) (16) + υ(SC) (7) + δ(SO_2—C3) (9) + δ(SO_2) (9)+δ(CCO) (8) + τ(OSN—H17) (24) + τ(OSNN) (13)
16	482	467	454	υ(SC) (4)+δ(CCO) (24) + δ(OSN) (10) + δ(CCN) (11) + δ(SNN) (5) + υ(SN) (16) + τ(OSN—H17) (8)
15		427	419	υ(SN) (8) + δ(SO_2) (16) + δ(OSN) (9) + τ(OSN—H17) (28) + τ(CNNH—17) (8) + τ(OSNN) (7)
14		404	395	υ(SC) (13) + υ(SN) (5) + δ(CC—C5) (22) + δ(NSC) (11) + τ(OSN—H17) (14) + τ(OSNN) (5)
13		355	348	υ(SN) (8) + δ(OSC) (26) + δ(CCO) (8) + τ(CSN—H15) (17) + τ(CSNN) (11) + τ(OSC—H9) (10)
12		339	327	δ(NCC) (29) + δ(CCC) (10) + δ(NCO) (9) + δ(NSO) (7) + δ(NNC) (6) + δ(CCO) (6)
11		294	288	υ(SN) (9) + δ(CSO) (11) + δ(NNS) (8) + δ(NNC) (7) + δ(NSO) (6) + τ(NNSO) (9) + τ(OSN—H17) (4)
10		260	254	δ(N—SO_2) (21) + δ(NS—O3) (9) + τ(CCNN) (10) + τ(CCN—H17) (5) + τ(OCNN) (4)
9		259	251	δ(CSO) (18) + τ(CC4—CH_3) (30) + τ(H6—C4—CH_3) (17)
8		212	205	δ(CCS) (18) + δ(CSN) (13) + δ(CCC) (11) + δ(NNC) (10) + τ(H8—C4—CH_3) (8) + τ(C3C4—CH_3) (16)
7		160	155	δ(NSC) (26) + δ(CCS) (17) + δ(NNC) (7) + δ(CSO) (6) + τ(C3C4—CH_3) (13)
6		116	114	δ(NNC) (5) + τ(CCCS)(16) + τ(SCC5—H8) (12) + τ(C4C3—SO_2) (9) + τ(CCC3—H9) (8) + τ(SCC4—H6) (7)
5		91	90	δ(NNS) (20) + τ(O1C2—CH_3) (23) + τ(CCNN) (21) + τ(OCNN) (16) + τ(SNNH17) (7) + τ(CNNH15) (6)
4		69	67	δ(NSC) (14) + τ(SNNC) (23) + τ(SNNH17) (12) + τ(NNSC) (11) + τ(CNNH15) (10) + τ(SCCC) (9)
3		51	50	τ(NC2—CH_3) (57) + τ(O1C2—CH_3) (10) + τ(NNCC) (9) + τ(NNSC) (5)
2		36	35	τ(NC2—CH_3) (19) + τ(CNNS) (14) + τ(CNNH15) (14) + τ(NN—SO_2) (12) + τ(NSCC) (7)
1		35	34	τ(NN—SO_2) (20) + τ(NSCC) (18) + τ(NNSC)(12) + τ(NSC—H10)(8) + τ(NSC—H9) (9) + τ(CSNH15) (8)

ν: bond stretching, δ: in-plane angle bending, γ: out-of-plane angle bending, sci: scissoring, tw: twisting, w: wagging, ρ: rocking, τ: torsion, as: antisymmetric and s: symmetric.

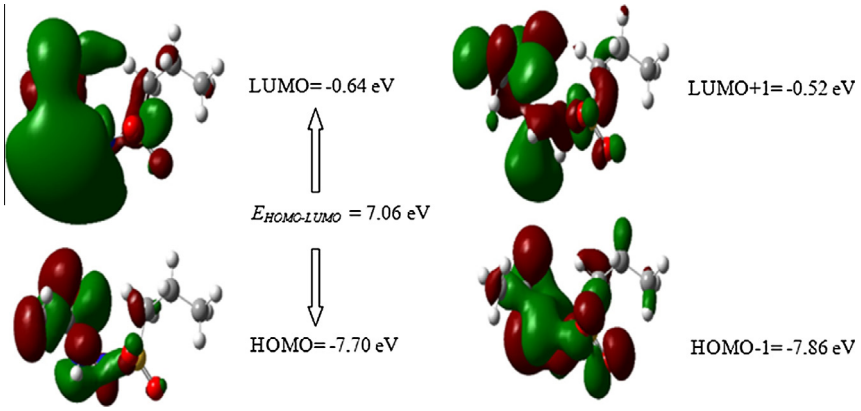

Fig. 3. Molecular orbital surfaces and energy levels for the HOMO-1, HOMO, LUMO and LUMO + 1 of *Apsh*.

Table 4
Experimental and calculated ^{13}C NMR and ^{1}H NMR chemical shifts (ppm) for *Apsh*.

Assignment	^{1}H NMR		Assignment	^{13}C NMR	
	Experimental	Calculated		Experimental	Calculated
C(1)**H$_3$**	1.82	1.79	**C1**	17.04	19.56
C(3)**H$_2$**	2.98	3.44	**C2**	169.28	171.52
C(5)**H$_3$**	1.95	1.89	**C3**	53.50	68.58
C(4)**H$_2$**	0.85	1.07	**C4**	13.02	12.52
N(1)**H**	9.27	7.47	**C5**	20.27	19.83
N(2)**H**	9.97	5.67			

Nonlinear optical (NLO) activity

Molecular materials with nonlinear optical (NLO) properties are currently attracting considerable attention because of their potential applications in optoelectronic devices of telecommunications, information storage, optical switching, and signal processing [39,40] and THz wave generation [41]. The dipole moment (μ), the static polarizability (α_0) and first static hyperpolarizability (β_{tot} are related directly to the non linear optical activity of structures) (Table 5).

The calculated values of the polarizabilities and the hyperpolarizabilities from Gaussian 03 output have been converted from atomic units into electrostatic units (α: 1a.u = 0.1482 $*$ 10^{-24} esu; β: 1a.u = 8.6393 $*$ 10^{-33} esu) [42].

The total static dipole moment μ, is defined as

$$\mu = \left(\mu_x^2 + \mu_y^2 + \mu_z^2\right)^{1/2}.$$

The calculations of static polarizability (α_{ave}) and first static hyperpolarizability (β_{tot}) from the Gaussian output have been stated in detail previously [43] as follows

$$\langle\alpha\rangle = 1/3(\alpha_{xx} + \alpha_{yy} + \alpha_{zz})$$

$$\beta_{tot} = \left[\left(\beta_{xxx} + \beta_{xyy} + \beta_{xzz}\right)^2 + \left(\beta_{yyy} + \beta_{yzz} + \beta_{yxx}\right)^2 + \left(\beta_{zzz} + \beta_{zxx} + \beta_{zyy}\right)^2\right]^{1/2}$$

The calculated first static hyperpolarizability (β_{tot}), mean polarizability ($\langle\alpha\rangle$) and the ground state dipole moment (μ) of the title compound are computed to be 1025.91 $\times$ 10^{-33} esu, 15.88 $\times$ 10^{-24} esu and 2.27 Debye, respectively. There are inverse relationship between first static hyperpolarizability and optical band gap($E_{HOMO-LUMO}$). While the optical band gap is too large (7.06 eV), the first static hyperpolarizability is too low (β_{tot} = 1025.91 $\times$ 10^{-33} esu). According to these results, the *Apsh*

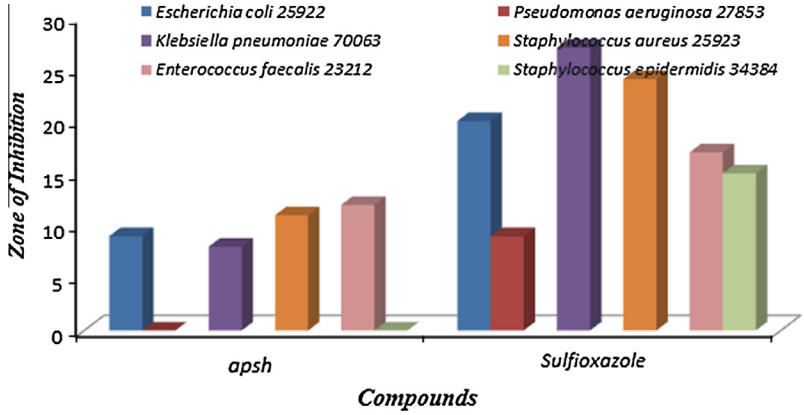

Fig. 4. Comparison of antibacterial activite of Apsh and antibiotics.

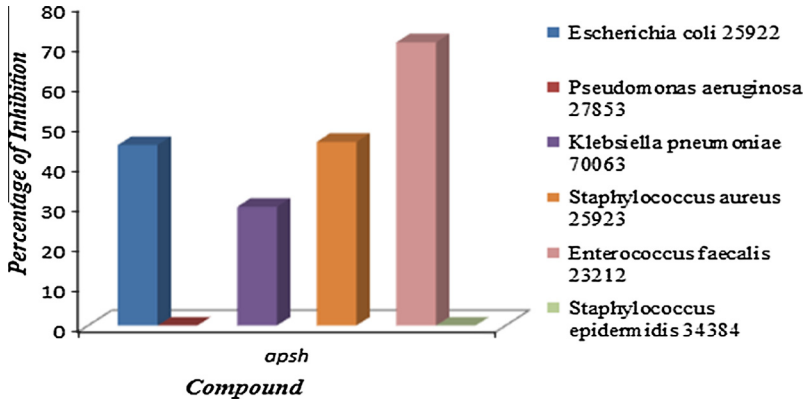

Fig. 5. Percentage of inhibition of Apsh against sulfisoxazol.

Table 5
The electric dipole moment μ (D), the mean polarizability $\langle\alpha\rangle$($\times 10^{-24}$ esu) and the first hyperpolarizability β_{tot} ($\times 10^{-33}$ esu) of the Apsh by DFT B3LYP/6-311++G(d,p) method.

Parameter	Value	Parameter	Value
μ_x	−2.03	β_{xxx}	−72.78
μ_y	0.70	β_{xxy}	386.76
μ_z	0.74	β_{xyy}	700.18
μ	2.27	β_{yyy}	210.68
α_{xx}	18.81	β_{xxz}	264.54
α_{xy}	−0.25	β_{xyz}	105.07
α_{yy}	15.31	β_{yyz}	121.57
α_{xz}	−0.80	β_{xzz}	−88.17
α_{yz}	−0.14	β_{yzz}	−66.62
α_{zz}	13.51	β_{zzz}	−215.32
$\langle\alpha\rangle$	15.88	β_{tot}	1025.91

α: 1a.u = $0.1482 * 10^{-24}$ esu.
β: 1a.u = $8.6393 * 10^{-33}$ esu.

molecule presents low nonlinear optical activity. However, addition of the molecules to the ends of drawing and withdrawing group nonlinear optical activity can be increased.

Antibacterial activity results

The test compound was screened in vitro for their antibacterial activity against three Gram-positive species (*S. epidermidis, S. aureus, E. faecalis)* and three Gram-negative species (*E. coli, P. aeruginosa, K. pneumoniae*) of bacterial strains by the disc diffusion and micro dilution methods. The antibacterial results were given in Table 6 by disc diffusion and Table 7 micro dilution methods. The results was compared with those of the standard drug sulfioxazole (Figs. 4 and 5).

The size of the inhibition zone depends upon the culture medium, incubation conditions, rate of diffusion and the concentration of the antibacterial agent (the activity increases as the concentration increases). In the present study, the Apsh is active against two *Gram-negative bacteria; E. coli*, *K. pneumoniae* and two *Gram-positive* bacteria; *S. aureus, E. faecalis* which may indicate broad-spectrum properties. Apsh show the highest activities against Gram-positive *bacteria E. faecalis* in the diameter zone of 12 mm whereas Gram-negative *bacteria P. aeruginosa and* Gram-positive *bacteria S. epidermidis* have been found inactive (Table 6). Percentage of inhibition for the compound exhibited in Fig. 5. As seen in Fig. 5, Apsh has moderate activity against *E. faecalis* whereas rest of the bacterias show weak activity.

According to the MIC's results shown in Table 7, the compound possess a broad spectrum of activity against the tested bacteria at the concentrations of 375– (>1500) μg/mL. MIC's results also showed that the Apsh is active agains two *Gram-negative bacteria; E. coli*, *K. pneumoniae* and two *Gram-positive* bacteria; *S. aureus, E. faecalis.*

LUMO energy is one of the most important descriptors which describe electrophilicity of the compound and its level has the importance because of the donor–acceptor interactions.

Table 6
Measured inhibition zone diameter (mm) of the compound (150 μg/mL) and antibiotics by disc diffusion method.

Compound	*Gram-negative*			*Gram-positive*		
	E. coli ATCC 25922	*P. aeruginosa* ATCC 27853	*K. pneumoniae* ATCC 70063	*S. aureus* ATCC 25923	*E. faecalis* ATCC 23212	*S. epidermidis* ATCC 34384
Apsh	9	–	8	11	12	–
Sulfisoxazole	20	9	27	24	17	15

Sulfisoxazole(300 μg/disk)<10: weak; >10 moderate; >16: significant.

Table 7
The MICs of antibacterial activity of the Apsh.

Compounds	MIC μg/mL					
	Gram-negative			*Gram-positive*		
	E. coli ATCC 25922	*P. aeruginosa* ATCC 27853	*K.pneumoniae* ATCC 70063	*S. aureus* ATCC 25923	*E. faecalis* ATCC 23212	*S. epidermidis* ATCC 34384
Apsh	375	>1500	375	375	375	>1500
Sulfisoxazole	23.4	375	23.4	23.4	93.75	93.75

Generally, molecules with a low LUMO energy values accept the electrons more easily than higher's. The low LUMO energy and larger $E_{HOMO-LUMO}$ band gap affect the binding affinities to the biologic molecules, therefore LUMO energy and $E_{HOMO-LUMO}$ band gap are important factors for N'-Acetyl propane sulfonic acid hydrazide activities. The biological activity of the N'-Acetyl propane sulfonic acid hydrazide increases with the lower LUMO energy, lower nonlinear optical activity ($\beta_{tot} = 1025.91 \times 10^{-33}$ esu) and bigger $E_{HOMO-LUMO}$ gap. Similar results were also reported by us [44–47].

Conclusions

In this study, we have reported the synthesis of Apsh. The structural characterization of the synthesized compound was made by using the elemental analyses and spectroscopic methods. The structure of N'-Acetyl propane sulfonic acid hydrazide (Apsh) was also supported by X-ray crystal diffraction studies. A complete vibrational analysis was also performed within the SQM-FF method the great match between experimental and calculated vibrational wavenumbers. While the optical band gap is too large, nonlinear optical activity of Apsh is too low. However, nonlinear optical activity of Apsh can be increased by adding donor and acceptor fragments to the ends of the molecule. Apsh showed the highest activities against Gram-positive *bacteria E. faecalis*.

Appendix A. Supplementary material

CCDC 1003393 contain the supplementary crystallographic data for compound. This data can be obtained free of charge from The Cambridge Crystallographic Data Centre via www.ccdc.cam.ac.uk/data_request/cif. [Fax: int code +44(1223) 336-033; e-mail: deposit@ccdc.cam.ac.uk].

References

[1] G. Domagk, Deut. Med. Wochenschr. 61 (1935) 250–258.
[2] G.L. Mandell, W.A. Petri, J.G. Hardman, L.E. Limbird, P.B. Molinoff, R.W. Ruddon, A.G. Gilman, Goodman's and Gilman's the Pharmacological Basis of Therapeutics, ninth ed., McGraw-Hill, New York, 1996, pp. 1073–1101.
[3] X. He, L. Tang, L. He, P. Xu, Huaxi Yike Daxue Xuebao 19 (1988) 317–322.
[4] T. Nogrady, Medicinal Chemistry, second ed., Oxford University Press, New York, 1988, p. 383.
[5] M.E. Wolff, fifth ed., Burger's Medicinal Chemistry and Drug Discovery, vol. 2, Wiley, Laguna Beach, 1996, pp. 528–576.
[6] S. Alyar, N. Karacan, J. Enzym. Inhib. Med. Chem. 24 (2009) 986–992.
[7] N. Özbek, H. Katırcıoglu, N. Karacan, T. Baykal, Bioorg. Med. Chem. 15 (2007) 5105–5109.
[8] S. Alyar, N. Ozbek, N. Karacan, Drug Future 32 (2007) 126–127.
[9] N. Özbek, S. Alyar, N. Karacan, Drug Future 32 (2007) 127–128.
[10] A. Ienco, C. Mealli, P. Paoli, N. Dodoff, Z. Kantarci, N. Karacan, New J. Chem. 23 (1999) 1253–1260.
[11] N. Özbek, S. Alyar, N. Karacan, J. Mol. Struct. 938 (2009) 48–53.
[12] U. Ozdemir, F. Arslan, F. Hamurcu, Spectrochim. Acta, Part A 75 (2010) 121–126.
[13] U.O. Ozdemir, N. Akkaya, N. Ozbek, Inorg. Chim. Acta 400 (2013) 13–19.
[14] S. Sert, O.S. Şentürk, U.O. Ozdemir, N. Karacan, F. Uğur, J. Coord. Chem. 57 (2004) 183–188.
[15] U. Ozdemir, O.S. Şentürk, S. Sert, N. Karacan, F. Uğur, J. Coord. Chem. 59 (2006) 1905–1911.
[16] G.M. Sheldrick, SHELXS97 and SHEXL97. Program for Crystal Structure Solution and Refinement. University of Göttingen, Germany, 1997.
[17] L.J. Farrugia, J. Appl. Cryst. 30 (1997) 565.
[18] M.J. Frisch, G.W. Trucks, H.B. Schlegel, G.E. Scuseria, M.A. Robb, J.R. Cheeseman, J.A. Jr. Montgomery, T. Vreven, K.N. Kudin, J.C. Burant, J.M. Millam, S.S. Iyengar, J. Tomasi, V. Barone, B. Mennucci, M. Cossi, G. Scalmani, N. Rega, G.A. Petersson, H. Nakatsuji, M. Hada, M. Ehara, K. Toyota, R. Fukuda, J. Hasegawa, M. Ishida, T. Nakajima, Y. Honda, O. Kitao, H. Nakai, M. Klene, X. Li, J.E. Knox, H.P. Hratchian, J.B. Cross, C. Adamo, J. Jaramillo, R. Gomperts, R.E. Stratmann, O. Yazyev, A.J. Austin, R. Cammi, C. Pomelli, J.W. Ochterski, P.Y. Ayala, K. Morokuma, G.A. Voth, P. Salvador, J.J. Dannenberg, V.G. Zakrzewski, S. Dapprich, A.D. Daniels, M.C. Strain, O. Farkas, D.K. Malick, A.D. Rabuck, K. Raghavachari, J.B. Foresman, J.V. Ortiz, Q. Cui, A.G. Baboul, S. Clifford, J. Cioslowski, B.B. Stefanov, G. Liu, A. Liashenko, P. Piskorz, I. Komaromi, R.L. Martin, D.J. Fox, T. Keith, M.A. Al-Laham, C.Y. Peng, A. Nanayakkara, M. Challacombe, P.M.W. Gill, B. Johnson, W. Chen, M.W. Wong, C. Gonzalez, J.A. Pople Gaussian 03: Revision D.01 Gaussian, Inc., Pittsburgh, PA, 2003.
[19] P.C. Hariharan, J.A. Pople, J. Chem. Phys. 27 (1974) 209–214.
[20] A.W. Bauer, W.M. Kirby, J.C. Sherris, M. Turck, Am. J. Clin. Pathol. 45 (1966) 493–496.
[21] G. Küçükgüzel, A. Kocatepe, E.D. Clercq, F. Şahin, M. Güllüce, Eur. J. Med. Chem. 41 (2006) 353–359.
[22] Ü. Özmen Özdemir, E. Aktan, F. Ilbiz, A. Balaban Gündüzalp, N. Özbek, M. Sarı, Ö. Çelik, S. Saydam, Inorg. Chim. Acta 423 (2014) 194–203.
[23] U. Ozdemir, P. Güvenç, E. Şahin, F. Hamurcu, Inorg. Chim. Acta 362 (2009) 2613–2618.
[24] S. Alyar, U.O. Ozmen, N. Karacan, O.S. Şentürk, K.A. Udachin, J. Mol. Struct. 889 (2008) 144.
[25] G. Fogarasi, P. Pulay, Ab initio calculation of force fields and vibrational spectra, Vibrational Spectra and Structure: a Series of Advances, vol. 14, Elsevier, Amsterdam, 1985, pp. 125–219 (Chapter 3).
[26] H. Alyar, A. Ünal, N. Özbek, S. Alyar, N. Karacan, Spectrochim. Acta A 91 (2012) 39.
[27] SQM version 1.0, Scaled Quantum Mechanical, 2013 Green Acres Road, Fayetteville, Arkansas 72703, 2013.
[28] N. Ozbek, H. Katircioglu, N. Karacan, T. Baykal, Bioorg. Med. Chem. 15 (2007) 5105–5109.
[29] K. Hanai, T. Okuda, T. Uno, K. Machida, Spectrochim. Acta 31A (1975) 1217–1225.
[30] R.D. Bindal, J.T. Golab, J.A. Katzenellenbogen, J. Am. Chem. Soc. 112 (1990) 7861–7868.
[31] N.I. Dodoff, Int. J. Vib. Spectrosc. 3 (1999) 7.
[32] L. Szabo, V. Chis, A. Pirnau, N. Leopold, O. Cozar, S. Orosz, Vib. Spectrosc. 48 (2008) 297–301.
[33] N.P.G. Roeges, A Guide to the Complete Interpretation of Infrared Spectra of Organic Structures, Wiley, New York, 1994.
[34] R.M. Silverstein, F.X. Webster, Spectrometric Identification of Organic Compounds, sixth ed., Wiley, Asia, 2003.
[35] Y. Tanaka, Y. Tanaka, Chem. Pharm. Bull. 13 (1965) 858–861.
[36] F. Blanco, I. Alkorta, J. Elguero, Magn. Reson. Chem. 45 (2007) 797–800.
[37] A.M.S. Silva, R.M.S. Sousa, M.L. Jimeno, F. Blanco, I. Alkorta, J. Elguero, Magn. Reson. Chem. 46 (2008) 859–864.
[38] I. Fleming, Frontier Orbitals, Organic Chemical Reactions, John Wiley and Sons, New York, 1976.
[39] P.N. Parasad, D.J. Williams, Introduction to Nonlinear Optical Effects in Molecules and Polymers, JohnWiley & Sons, New York, 1991.
[40] F. Kajzar, K.S. Lee, A.K.-Y. Jen, Adv. Polym. Sci. 161 (2003) 1–5.
[41] V. Krishnakumar, R. Nagalakshmi, Physica B 403 (2008) 1863–1869.
[42] N. Sundaraganesan, E. Kavitha, S. Sebastian, J.P. Cornard, M. Martel, Spectrochem. Acta Part A 74 (2009) 788–797.
[43] H. Alyar, Z. Kantarci, M. Bahat, E. Kasap, J. Mol. Struc. 834–836 (2007) 516–520.
[44] S. Alyar, Ş. Adem, Spectrochim. Acta A 131 (2014) 294–302.
[45] S. Alyar, N. Özbek, S.Ö. Yıldırım, S. İde, R.J. Butcher, Spectrochim. Acta A 130 (2014) 198–207.
[46] U. Ozmen Ozdemir, A. Altuntaş, A. Balaban Gündüzalp, F. Arslan, F. Hamurcu Spectrochim. Acta, Part A 128 (2014) 452.
[47] A.B. Gündüzalp, U.O. Ozmen, B.S. Çevrimli, S. Mamaş, S. Çete, Med. Chem. Res. 23 (2014) 3255.